IEEE Access
Multidisciplinary | Rapid Review | Open Access Journal

Received September 26, 2018, accepted October 10, 2018, date of publication October 24, 2018,
date of current version November 30, 2018.

Digital Object Identifier 10.1109/ACCESS.2018.2877778

3D Vehicle Model Retrieval Method Based on Angle Structure Feature of Render Image

ZHI LIU, XIAOBIN PAN, AND GUOJIANG SHEN
College of Computer Science and Technology, Zhejiang University of Technology, Hangzhou 310023, China
Corresponding author: Guojiang Shen (gjshen1975@zjut.edu.cn)

This work was supported by the Natural Science Foundation of Zhejiang Province under Grant LY16F020033 and LY18F020032.

ABSTRACT In order to make full use of the color, shape, texture, and other features in the 3-D vehicle model, a 3-D vehicle model retrieval method is proposed based on angle structure features using render images as dataset. First, the 3-D vehicle model render images are taken as a testing set and the marked natural images are taken as a training set. The render images are classified based on their skeleton-associated shape context and the angle structure features are extracted to establish the feature library. Then, the angle structure features of the input natural image are extracted. The distance measure method is used to calculate the similarity between the angle structure feature of input natural image and those features in the feature library in order to achieve the 3-D vehicle model retrieval. The experimental results show that this retrieval method can effectively improve retrieval performance for the 3-D vehicle model.

INDEX TERMS 3D vehicle model retrieval, angle structure feature, render image, skeleton-associated shape context.

I. INTRODUCTION

The 3D model has been widely used in many fields such as industrial product design, virtual reality, 3D games, film, and television animation. With the increasing number of 3D models, it becomes urgent issue how to retrieve the most similar 3D model from the large number of existing 3D models faster and better.

Currently, the main content-based 3D model retrieval methods include 3D model retrieval based on sketches, 2D projection views, and case models. Among the related studies based on the sketches and two-dimensional projection views, Yoon *et al.* [1] proposed the use of diffusion tensor field for feature analysis of input sketches and projected contours, and used the histogram of oriented gradient to achieve similarity calculation. Lei *et al.* [2] proposed to integrate skeleton and contour features of sketches and projection views to achieve retrieval. Both of these methods are mainly focused on the using of shape information of sketch and view, and not using of information such as textures and colors effectively.

Visual information such as color, texture, and shape, which are widely used in graphic image retrieval methods, has also been applied to 3D model retrieval [3]–[8]. Pasqualotto *et al.* [9] proposed to use mesh image descriptors to obtain shape and color information of 3D model to achieve retrieval. It used shape information of 3D model while not ignoring the application of color information. Biasotti *et al.* [10] analyzed and compared six kinds of texture 3D shape retrieval and classification methods, and experimentally verified the feasibility of combining the three visual information of geometry shape, texture, and color to achieve 3D model retrieval.

Reference [11] proposed to use the microstructure descriptor to extract the underlying microscopic structure of similar edge orientation of the local image block, and used it as a bridge to integrate the color, texture, shape and color distribution information to describe the image. Reference [12] proposed to use a significant structural histogram to describe the image. Reference [13] proposed the angle structure feature concept. In this way, after an image was quantized by the color, the similarity calculation was performed by counting the number of angles and size relationships between adjacent pixel points in all local blocks. In the process of image retrieval, the angle structure features had strong recognition ability.

Because the 3D model render image fully reflects the color, shape, space and other characteristic information of 3D model, this paper proposes a 3D vehicle model retrieval method based on the angle structure of the render image. In this method, the 3D vehicle model render images are taken

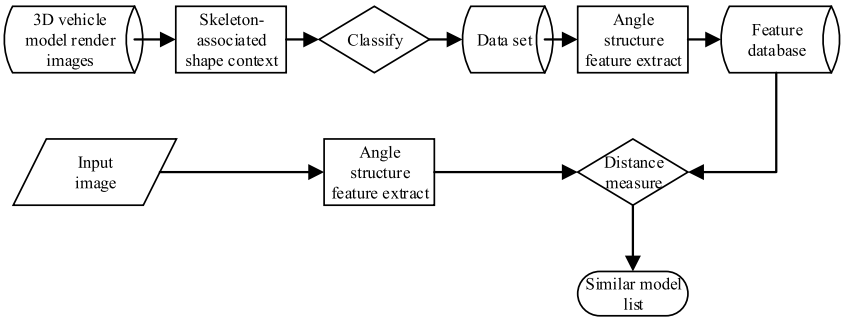

FIGURE 1. Framework of the 3D vehicle model retrieval algorithm.

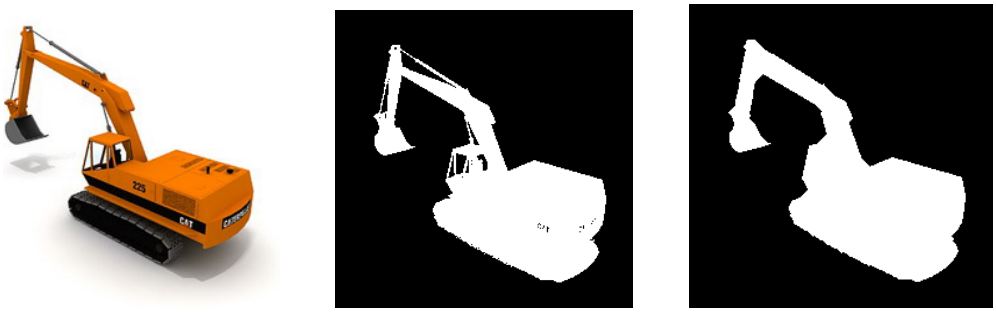

FIGURE 2. Binary image optimization. The first image is the original image, the second image is the first processed binary image and the last image is the second processed binary images.

as a testing set, the marked natural images are taken as a training set. The render images are classified by multi-category linear SVM and the angle structure features are extracted to establish the feature library. Then the similarity between the angle structure features of the input natural images and those features in the feature library will be calculated in order to retrieve 3D vehicle models.

II. ALGORITHM FRAMEWORK

In this paper, it is divided into two parts: firstly, it obtains the 3D vehicle models and render images from the Internet. Then using the marked natural image from the Internet as the training set, we train a multi-class linear SVM classifiers based on skeleton-associated shape context feature to achieve render images classification to form dataset. We extracted angle structure features of the render images to establish feature database. Finally, we extract angle structure feature of natural images on the Internet to realize 3D vehicle model retrieval based on distance measurement method. The algorithm framework is shown in Fig.1.

III. RENDER IMAGE CLASSIFICATION

This section mainly discusses render images classification through skeleton-associated shape context feature [14].

Firstly, the render images are binarized. Then the skeleton images can be obtained by using the algorithm put forward by Shen *et al.* [15]. It will find the nearest skeleton point for each contour point and the distance between two points is assigned to contour point. It is the combination of contour and skeleton information. Then it computes segmented skeleton-associated shape context feature and forms eigenvector based on skeleton-associated shape context features. Finally, the existing marked natural images from the Internet are taken as the training set. A multi-class linear SVM [16]–[19] as a classifier based on skeleton-associated shape context feature will be trained to classify render images and achieve 3D vehicle model classification.

A. SKELETON DIAGRAM EXTRACTION

Before extracting the skeleton image of the render image, it needs to be binarized and preprocessed firstly. However, the binary image still can be partially shaded. The binary image with partial shading may not get a good skeleton. Therefore, in order to get a better skeleton image, we need to erode and dilate the binary image twice to eliminate the excess shadow for the final binary image (as shown in Fig.2).

Shen *et al.* [15] proposed a method for extracting skeletons. It obtained the skeleton graph based on the commonly used skeleton algorithm. And it used the formula (1) to calculate the weights of the end branches of each segment of the skeleton. Then, it deleted the end branch with the lowest weight to achieve the purpose of trimming the skeleton to form a concise skeleton diagram (as shown in Fig.3). So the shape features of the image can be better expressed.

$$w_j^i = \alpha \frac{\Lambda(D - R(S^i - E_j^i))}{\Lambda(D)} + \log(\Gamma(S^i - E_j^i) + 1) \quad (1)$$

$$\alpha = \beta \log(\frac{\Gamma(M)}{\varpi(M)}), \quad S^0 = M,\ S^{i+1} = S^i - E_i \quad (2)$$

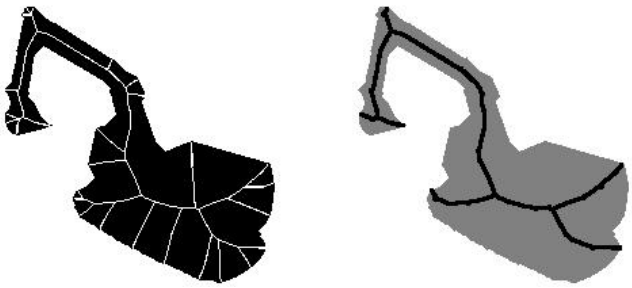

FIGURE 3. Skeleton diagram optimization. The first one was obtained through the common skeleton algorithm. The second one was obtained through the method of Shen et al. [15].

Where D is a set of shape contour points. S is a set of skeleton points and its superscript indicates the number of iterations. E is a set of end branch nodes and its superscript is same to S and its subscript indicates the number of end branch. α is the normalization factor. β is a constant 9. $\varpi(M)$ indicates the average length of the end path M. R represents the skeleton points reconstructed(they are the skeleton points after the end branch is deleted). Γ represents the normalized curve length. Λ indicates the area in pixels.

B. SKELETON-ASSOCIATED SHAPE CONTEXT FEATURE EXTRACTION

The shape context feature vector only contains the contour information. Here, the skeleton-associated shape context feature vector with the skeleton information can describe the shape of the object more comprehensively by combing the contour and skeleton information.

Skeleton-associated shape context is obtained by adding skeleton information based on shape context of contour points in the image [20], [21] (It adds skeleton information to contour points before calculating shape context of contour points. So that contour points have not only position information but also distance information from the contour point to the nearest skeleton point). The histogram is transformed from the 60-dimensional shape context (12 numbers for angle, 5 numbers for radius) to the 300-dimensional skeleton-associated shape context (12 numbers for the angle, 5 numbers for the radius, 5 numbers for the skeleton value). Then contour points containing skeleton information are segmented to obtain skeleton-associated shape context among five contour points in each segment to form 1500-dimensional skeleton-associated shape context eigenvector set. The feature packets are encoded to obtain the skeleton-associated shape context eigenvector set. It is shown in Fig.4.

C. RENDER IMAGE CLASSIFICATION

The natural images can be captured with category label as the training set online. Skeleton- associated shape context eigenvector set of the training set is obtained by the method in Section B, then a multi-class linear SVM is trained as a classifier[16], [17], as in

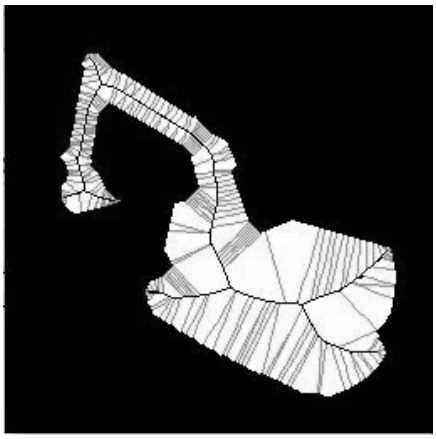

FIGURE 4. Skeleton-associated shape context.

$$\min_{w_1,\ldots,w_L} \sum_{j=1}^{M} ||w_j||^2 + \gamma \sum_{i} \max(0, 1 + w_{l_i}^T g_i - w_{y_i}^T g_i) \quad (3)$$

$$l_i = \arg\max_{l\in\{1,2,\ldots,L\}, l\neq y_i} w_l^T g_i \quad (4)$$

Here, a multi-category SVM classifier can be trained through the formula (3) on the training set. Then images in the testing set can be classified through formula (4). In formula (3), the first item is a regular term that is used to maximize the spacing of hyperplane. The second is the hinge loss function, which measures the quality of the predictor for classification prediction of input data. γ is a regularization constant used for balancing the regular term (left) and the hinge loss function (right). It is defined as a constant of 10. M represents the training images of all categories. g_i is the eigenvector set of training image. y_i is the class label of training image.

We use the render images of 3D vehicle models as the testing set. Firstly, we obtain the skeleton-associated shape context eigenvector set from the testing set by the method of Section B. Then we obtain the testing image category label $\widehat{y}$ based on the classifier in the formula (5). Finally according to the category label of the testing set, the render images and three-dimensional models with the same type are moved to the same folder to finish the classification of the 3D vehicle model indirectly and establish a better data set.

$$\widehat{y} = \arg \max_{l\in\{1,2,\ldots,L\}} w_l^T g \quad (5)$$

Where the g is eigenvector of testing image.

IV. 3D VEHICLE MODEL RETRIEVAL

Firstly, all of the render images in the data set will be quantized based on color. Then the angle structure features of the render images are extracted to build a feature library. Finally, the angle structure features of the input images are extracted to retrieve the similar vehicle model among the feature library with distance measurement method and realize the 3D vehicle model retrieval.

A. RENDER IMAGE COLOR QUANTIZATION

Androutsos *et al.* experimentally divided the HSV color space roughly, the brightness is greater than 75% and the saturation is greater than 20% for the bright color region, the brightness is less than 25% for the black region, the brightness is greater than 75% and the saturation is less than 20% for the white region. Others are colored areas [22]. In order to reduce computational complexity and describe image color, shape and texture features better, the color space is quantified as 72 spaces [23]. Here $H \in [0, 360]$, $S \in [0, 1]$ and $V \in [0, 1]$. It is shown in Fig. 5.

$$H = \begin{cases} 0, & H \in [0,24] \cup [345,360] \\ 1, & H \in [25,49] \\ 2, & H \in [50,79] \\ 3, & H \in [80,159] \\ 4, & H \in [160,194] \\ 5, & H \in [195,264] \\ 6, & H \in [265,284] \\ 7, & H \in [285,344] \end{cases}$$

$$S = \begin{cases} 0, & S \in [0,0.15] \\ 1, & S \in (0.15,0.8] \\ 2, & S \in (0.8,1] \end{cases}$$

$$V = \begin{cases} 0, & V \in [0,0.15] \\ 1, & V \in (0.15,0.8] \\ 2, & V \in (0.8,1] \end{cases}$$

FIGURE 5. HSV color space quantization.

The H channel is divided into 8 areas, the S channel is divided into 3 areas, the V channel is divided into 3 areas, According to the difference of the S and V channels, the obtained quantification function is different, as in

$$P = Q_S Q_V H + Q_V S + V \tag{6}$$

Where Q_S is the digitized number of color space components S and Q_V is the digitized number of color space components V. Because S and V are quantized to 3 levels, so $Q_S = 3$, $Q_V = 3$. Finally, we can get the formula as in

$$P = 9H + 3S + V \tag{7}$$

Then the three channels of each pixel in the image are combined into a single value using the quantization function. The final image is described as a 2D matrix in which the position of each value in the matrix is one-to-one correspondence with the pixel position in the image and the value in the matrix is calculated through the quantization function.

Assuming that I is the original image before color quantization of the image. I is defined as a color-quantized value. Li iis a point whose value is a color-quantized value, which can be obtained from the formula (8)

$$L_i = \{(x, y) \mid (x, y) \in I, I(x, y) = i, 0 \le i \le 71\} \tag{8}$$

B. ANGLE STRUCTURE FEATURE EXTRACTION

It is mainly divided into the following three steps for the extraction of the angle structure feature:

1) For each quantized color α, we move 2 * 2 area starting with the coordinate (0,0) to go through the quantized color matrix from left to right and from top to bottom. In this process, the color matrix is divided into many 2 * 2 local blocks. For each local block, this local block is reserved if *V1* is the same as the current quantized color α, otherwise the local block is removed.

2) For the remaining blocks, we can obtain angle relationship between *V1* and *V2*, *V3*, *V4* in the same block (as shown in Fig.6)

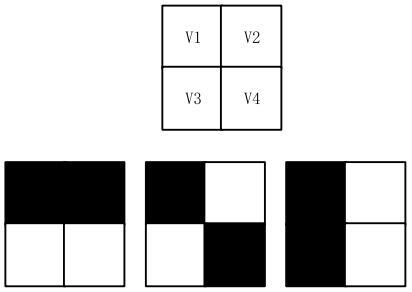

FIGURE 6. Angle structures with different orientations. The black-and-white block represents three different angle structures: 0^0, 45^0 and 90^0 angle structure respectively.

The value relationships between *V1* and *V2*, *V3*, *V4* in the same block are shown in Fig.7.

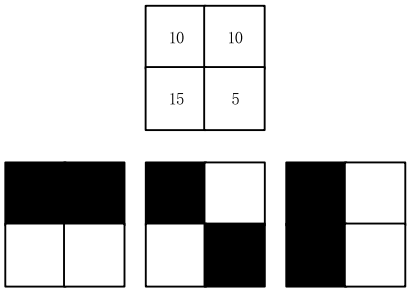

FIGURE 7. Value relationships based on different angle relationships. In second row, the first 2*2 block represents equal relationship at the 0^0 angle structure. The second 2*2 block represents greater relationship at the 45^0 angle structure. The third 2*2 block represents less relationship at the 90^0 angle structure respectively.

After counting the number of value relationship in all angles, it finally gets a 9-dimensional vector of color space. Where $N^E_{0^\circ}, N^L_{0^\circ}, N^G_{0^\circ}$ are the numbers of equal, less, and greater relationships in the 0^0 angle structure.

Similarly, $N^E_{45^\circ}, N^L_{45^\circ}, N^G_{45^\circ}$ and $N^E_{90^\circ}, N^L_{90^\circ}, N^G_{90^\circ}$ are the numbers in the 45^0 and 90^0 angle structure respectively.

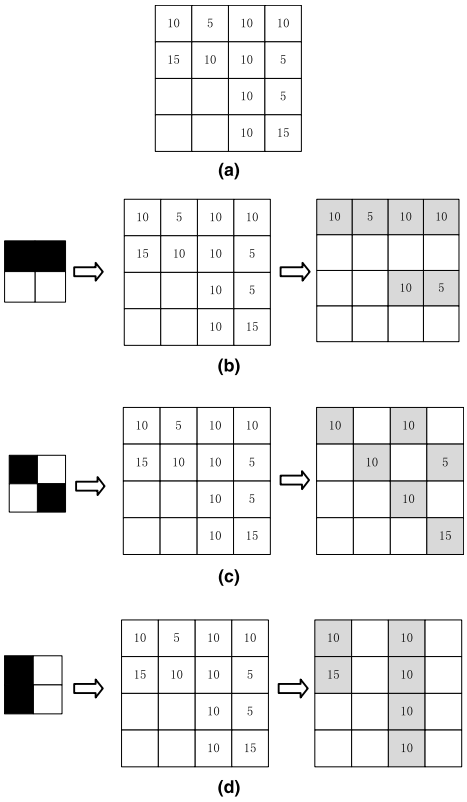

FIGURE 8. (a)Original image. (b) Value relationship at the 0^0 angle structure. (c) Value relationship at the 45^0 angle structure. (d) Value relationship at the 90^0 angle structure.

For example, using an image (as shown in Fig.8(a)) as the original image, a 9-dimensional vector (assuming the current quantized color value is 10) can be obtained

The 0^0 local block is used to scan the original image and the 0^0 image can be gotten. Here, there is one equal relationship, two greater relationships. There is no less relationship in the three blocks. So the value of $N_{0^\circ}^E$ is 1, the value of $N_{0^\circ}^L$ is 0, and the value of $N_{0^\circ}^G$ is 2. It is shown in Fig. 8(b).

The 45^0 local block is used to scan the original image and the 45^0 image can be gotten. Here, there is one equal relationship, one greater relationship, and one less relationship in the three blocks. So the value of $N_{45^\circ}^E$ is 1, the value of $N_{45^\circ}^L$ is 1, and the value of $N_{45^\circ}^G$ is 1. It is shown in Fig. 8(c).

The 90^0 local block is used to scan the original image and the 90^0 image can be gotten. Here, there are two equal relationships, and one less relationship. There is no greater relationship in the three blocks. So the value of $N_{90^\circ}^E$ is 2, the value of $N_{90^\circ}^L$ is 1, and the value of $N_{90^\circ}^G$ is 0. It is shown in Fig. 8(d).

So we can obtain the 9-dimensional vector of the original image:

$$(N_{0^\circ}^E, N_{0^\circ}^L, N_{0^\circ}^G, N_{45^\circ}^E, N_{45^\circ}^L, N_{45^\circ}^G, N_{90^\circ}^E, N_{90^\circ}^L, N_{90^\circ}^G) = (1, 0, 2, 1, 1, 1, 2, 1, 0)$$

3) In order to reduce the vector dimension, it defines $T = (t_1, t_2, t_3)$ to represent the angle structure.

Where t_1 is greater relationship, t_2 is less relationship, t_3 is equal relationship.

$T^E = (0, 0, 1)$, $T^L = (0, 1, 0)$ and $T^G = (1, 0, 0)$ represent equal, less and greater relationship respectively. T can be calculated by the formula as in (9).

$$T = \sum_{i=1}^{3} t_i 2^{(i-1)} \tag{9}$$

It defines $L_{\alpha_{0^\circ}}, L_{\alpha_{45^\circ}}, L_{\alpha_{90^\circ}}$ as the values of the three angle structures with the current quantized color value α, and the corresponding values are calculated by the formula as in (10). Taking 0^0 angle structure as an example,

$$L_{a_{0^\circ}} = T^E N_{0^\circ}^E + T^L N_{0^\circ}^L + T^G N_{0^\circ}^G \tag{10}$$

So, the 216-dimensional angle structure feature vector H of image can be gotten.

$$H = [L_{0_{0^\circ}}, L_{0_{45^\circ}}, L_{0_{90^\circ}}, \ldots\ldots, L_{\alpha_{0^\circ}}, L_{\alpha_{45^\circ}}, L_{\alpha_{90^\circ}}, \ldots\ldots, L_{71_{0^\circ}}, L_{71_{45^\circ}}, L_{71_{90^\circ}}]$$

Finally, we can extract angle structure features of the render images in the data set to establish a feature library.

C. SIMILARITY CALCULATION

Here, we extract angle structure features of natural images acquired on the Internet. Similar models are retrieved from the feature library using distance metrics and sorted by similarity.

We use the Manhattan distance, the Euclidean distance and the distance proposed by [13] to calculate the similarity and get the e-measures and second-tier of the search results respectively(as shown in Table 1). The AP in the three kinds of distances are shown in the Table 1.

TABLE 1. AP in the different distances.

Distance	ST	EM
Our Distance	0.326	0.188
Manhattan Distance	0.288	0.151
Euclidean Distance	0.300	0.162

Assuming that the feature vector of the input image is $Q = [Q_1, Q_2, \ldots, Q_L]$ and the feature vector of the image in the data set is $T = [T_1, T_2, \ldots, T_L]$. The distance between the two is obtained by the formula (11)

$$D(T, Q) = \sum_{i=1}^{L} \frac{|T_i - Q_i|}{1 + T_i + Q_i} \tag{11}$$

V. EXPERIMENTAL ANALYSIS

The method mentioned above is implemented on the Windows platform. Hardware configuration is the CPU Intel Core^{TM} i5-2450M and memory is 8G. The 3D vehicle models and corresponding render images in dataset used in this experiment are obtained and selected from three websites, such as

http://3dwarehouse.sketchup.com, htpp://artist −3d.com and http://archive3d.net. These 3D vehicle models are selected through text suffixes and keywords. The 3D vehicle models in dataset contain natural object properties and have good grid density.

A. EXPERIMENTAL SETUP

As the 17 different types of models used in [24], this paper also limits the experimental model categories to car, bus, SUV, bike, motorbike, truck, and excavator. The 40 natural images in 7 categories from the Internet as a training set are used in this paper. The eighteen 3D vehicle models and their render images in 7 categories acquired from the three websites above mentioned are used as testing set. The multi-category linear SVMs are trained as classifiers by using the skeleton shape context features in the training set and used to classify the render images in the testing set. We select 40 render images from each category after being classified as datasets, and then use online-access 20 natural images of 7 categories as input images, and finally use 216-dimensional angle structure features to perform image retrieval and achieve 3D vehicle model retrieval. All rendered images in the dataset are 128x128 or 230x130 jpg format images. All 3D vehicle model types include obj, off, and skp.

B. EXPERIMENTAL VERIFICATION ANALYSIS

In the process of retrieval, the color of the render image is quantified firstly. It can describe the color, shape and texture information of the image through quantifying. Then the angle structure is used to integrate the color, shape, texture and color spatial distribution information to create a 216-dimensional feature vector. Finally, the vector differences between the input images and the render images in dataset are compared through the distance measurement method to realize the 3D vehicle model retrieval. This paper makes full use of the information such as the color, shape, texture and color space of the render image to make up for the lack of information caused by the single render image.

To verify the search results, we selected one input image from three categories: car, bike, and excavator, and then retrieved the top 12 results. The results are shown in Fig. 9.

The experimental results that the natural image containing more visual information as input source, the method proposed here has better retrieval performance for the 3D vehicle models with different categories and forms.

C. COMPARATIVE EXPERIMENT

Under the same 7 categories of experimental data, a first-tiered (FT) evaluation index is used to compare horizontally with Gabor+BOW [24], as shown in Fig.10, the y-ordinate represents the size of First-Tier.

The experimental results show that the retrieval method used in this article has relatively good retrieval performance in more complex categories such as car, bus, SUV, truck, and excavator. However, in simple categories such as bike, motorbike, due to the relatively simple change of the angle structure relationship between adjacent pixels in the natural image and the render image, less visual information are extracted relatively. So the differentiation of the formed angle

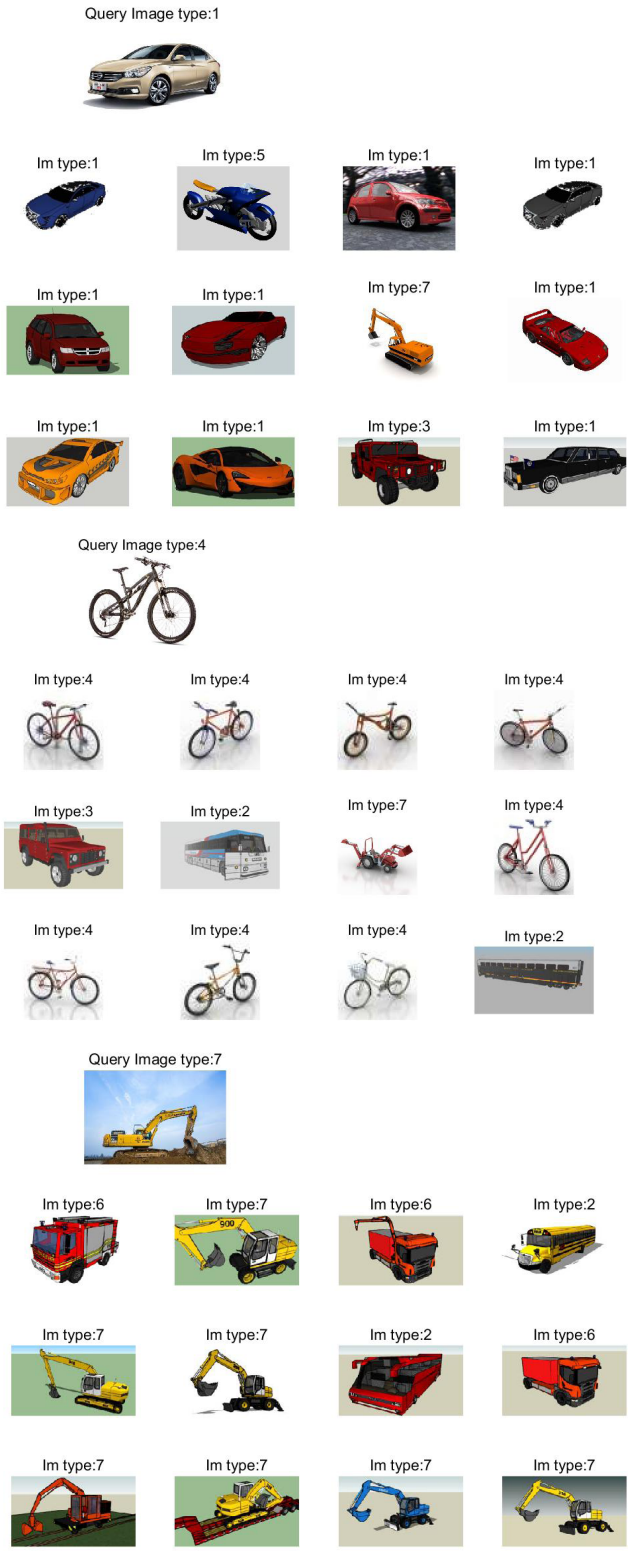

FIGURE 9. The 3D vehicle model retrieval results of car, bike and excavator using our method.

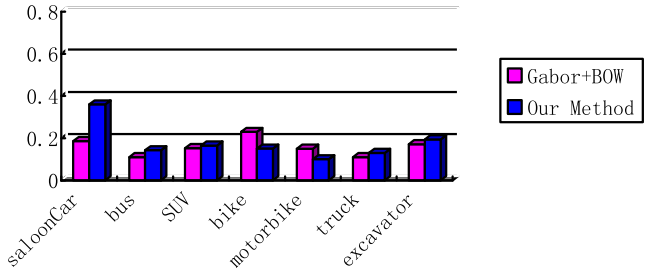

FIGURE 10. FT experimental contrast in some categories.

structure feature is reduced. It has some influence on the retrieval results. It also indicates the method in this paper can be further optimized.

In order to make the retrieval evaluation more comprehensive, the Second-Tier (ST), E-Measures (EM), Nearest Neighbor (NN), Normalized Discounted Cumulative Gain (nDCG) and Average Precision (AP) [25] are used to quantity experimental result (as shown in Table 2).

TABLE 2. Retrieval performance contrast table.

Indicators	Our Method	Gabor+BOW[19]
ST	0.326	0.297
EM	0.188	0.165
nDCG	0.183	0.172
NN	0.171	0.150
AP	0.242	0.186

VI. CONCLUSION

In this paper, a 3D vehicle model retrieval method based on angle structure features of render images is proposed. In this method, the color, shape and space information of the 3D vehicle model are fully utilized. A classifier based on the skeleton shape context feature is realized and used to classify the 3D model rendering images. Then the classified rendering images are taken as data set to establish angle structure feature library. Through calculating the similarity between the input images and the rendering images classified realizes the 3D vehicle model retrieval. It makes up the problem of insufficient information caused by a single render image effectively. The experimental results show that the proposed method has a good retrieval effect on the 3D vehicle models with complex angle structure changes among the adjacent pixels in the render images. Due to the quantity and quality of the render images of 3D vehicle models, the universality of this method is limited to some extent.

REFERENCES

[1] S. M. Yoon, M. Scherer, T. Schreck, and A. Kuijper, "Sketch-based 3D model retrieval using diffusion tensor fields of suggestive contours," in *Proc. 18th ACM Int. Conf. Multimedia*, Oct. 2010, pp. 193–200. [Online]. Available: https:// dl.acm.org /citation.cfm?id=1873961

[2] H. Lei, Y. Li, H. Chen, S. Lin, G. Zheng, and X. Luo, "A novel sketch-based 3D model retrieval method by integrating skeleton graph and contour feature," *J. Adv. Mech. Des., Syst., Manuf.*, vol. 9, no. 4, p. JAMDSM0049, 2015.

[3] J. Zhang, C. Bai, J. F. Nezan, and J.-G. Cousin, "Joint motion model for local stereo video-matching method," *Opt. Eng.*, vol. 54, no. 12, p. 123108, Dec. 2015.

[4] J. Zhang, J. Shang, and G. Zhang, "Verification for different contrail parameterizations based on integrated satellite observation and ECMWF reanalysis data," *Adv. Meteorol.*, vol. 2017, Oct. 2017, Art. no. 8707234, doi: 10.1155/2017/8707234.

[5] L. Li and Y. Liu, "Wavelet transform image retrieval method based on content," *Comput. Sci.*, vol. 42, no. 2, pp. 306–310, Feb. 2015.

[6] Z. AoBo, W. Xianbin, and X. Zhang, "Retrieval algorithm for texture image based on improved dual tree complex wavelet transform and gray gradient co-occurrence matrix," *Comput. Sci.*, vol. 44, no. 6, pp. 274–277, Jun. 2017.

[7] K. Seetharaman and N. Palanivel, "Texture characterization, representation, description, and classification based on full range Gaussian Markov random field model with Bayesian approach," *Int. J. Image Data Fusion*, vol. 4, no. 4, pp. 342–362, 2013.

[8] K. Seetharaman and M. Jeyakarthic, "Statistical distributional approach for scale and rotation invariant color image retrieval using multivariate parametric tests and orthogonality condition," *J. Vis. Commun. Image Represent.*, vol. 25, no. 5, pp. 727–739, 2014.

[9] G. Pasqualotto, P. Zanuttigh, and G. M. Cortelazzo, "Combining color and shape descriptors for 3D model retrieval," *Signal Process Image Commun.*, vol. 28, no. 6, pp. 608–623, Jul. 2013.

[10] S. Biasotti *et al.*, "Retrieval and classification methods for textured 3D models: A comparative study," *Vis. Comput.*, vol. 32, no. 2, pp. 217–241, Feb. 2016.

[11] G.-H. Liu, Z.-Y. Li, L. Zhang, and Y. Xu, "Image retrieval based on micro-structure descriptor," *Pattern Recognit.*, vol. 44, no. 9, pp. 2123–2133, 2011.

[12] G.-H. Liu, J.-Y. Yang, and Z. Y. Li, "Content-based image retrieval using computational visual attention model," *Pattern Recognit.*, vol. 48, no. 8, pp. 2554–2566, 2015.

[13] M. Zhao, H. Zhang, and L. Meng, "An angle structure descriptor for image retrieval," *China Commun.*, vol. 13, no. 8, pp. 222–230, Sep. 2016.

[14] W. Shen *et al.*, "Shape recognition by bag of skeleton-associated contour parts," *Pattern Recognit. Lett.*, vol. 83, no. 3, pp. 321–329, Nov. 2016.

[15] W. Shen, X. Bai, X. Yang, L. J. Latecki, "Skeleton pruning as trade-off between skeleton simplicity and reconstruction error," *Sci. China Inform. Sci.*, vol. 56, no. 4, pp. 1–14, Apr. 2013.

[16] K. Crammer and Y. Singer, "On the algorithmic implementation of multiclass kernel-based vector machines," *J. Mach. Learn. Res.*, vol. 2, pp. 265–292, Mar. 2001.

[17] R. Moore, J. Denero. (Jun. 2011). *L1 and L2 Regularization for Multi-class Hinge Loss Models. MLSLP*. [Online]. Available: http://www.ttic.edu/sigml/symposium2011/papers/Moore+DeNero_Regularization.pdf

[18] X. J. Kong *et al.*, "Mobility dataset generation for vehicular social networks based on floating car data," *IEEE Trans. Veh. Technol.*, vol. 67, no. 5, pp. 3874–3886, May 2018, doi: 10.1109/TVT.2017.2788441.

[19] W. Hou, Z. Ning, L. Guo, and X. Zhang, "Temporal, functional and spatial big data computing framework for large-scale smart grid," *IEEE Trans. Emerg. Topics Comput.*, to be published, doi: 10.1109/TETC.2017.2681113.

[20] X. Bai, W. Liu, and Z. Tu, "Integrating contour and skeleton for shape classification," in *Proc. IEEE 12th Int. Conf. Comput. Vis. Workshops (ICCV Workshops)*, Sep./Oct. 2009, pp. 360–367. [Online]. Available: https://pdfs.semanticscholar.org/1965/d791ff65db81ae08b968ae55a6d4755e18e0.pdf

[21] W. Shen, X. Wang, C. Yao, and X. Bai, "Shape recognition by combining contour and skeleton into a mid-level representation," in *Proc. Chin. Conf. Pattern Recognit.*, 2014, pp. 391–400. [Online]. Available: https://pdfs.semanticscholar.org/590a/d3e37a89132c7b983af15c79c8a405a7ba11.pdf.X

[22] D. Androutsos, K. N. Plataniotis, and A. N. Venetsanopoulos, "Vector angular distance measure for indexing and retrieval of color," *Proc. SPIE*, vol. 3656, pp. 604–613, Dec. 1999.

[23] X. Wang and Z. Wang, "A novel method for image retrieval based on structure elements' descriptor," *J. Vis. Commun. Image Represent.*, vol. 24, no. 1, pp. 63–74, 2013.

[24] Z. Liu, Y. Shichao, P. Xiang, and Z. Herong, "3D model retrieval method based on feature lines," *J. Comput.-Aided Des. Comput. Graph.*, vol. 28, no. 9, pp. 1512–1520, Sep. 2016.
[25] P. Shilane, P. Min, M. Kazhdan, and T. Funkhouser, "The princeton shape benchmark," in *Proc. Shape Modeling Appl.*, Jun. 2014, pp. 167–178. [Online]. Available: http://shape.cs.princeton.edu/benchmark/benchmark.pdf

ZHI LIU received the B.S. degree in automatic control and the M.S. degree in system engineering from Xi'an Jiaotong University, Xi'an, China, in 1991 and 1994, respectively, and the Ph.D. degree in computer application from Zhejiang University, Hangzhou, China, in 2001. She is currently a Professor with the College of Computer Science and Technology, Zhejiang University of Technology, Hangzhou, China. Her research interests mainly include 3-D model retrieval, image processing, and intelligent transportation system. She is a member of the China Computer Federation.

XIAOBIN PAN received the B.S. degree in computer science and technology from the Anhui University of Technology, Maanshan, China, in 2015, and the M.S. degree in computer science and technology from the Zhejiang University of Technology, Hangzhou, China. His research interests include 3-D model retrieval and image processing.

GUOJIANG SHEN received the B.Sc. degree in control theory and control engineering and the Ph.D. degree in control science and engineering from Zhejiang University, Hangzhou, China, in 1999 and 2004, respectively. He is currently a Professor with the College of Computer Science and Technology, Zhejiang University of Technology, Hangzhou, China. His current research interests include artificial intelligence, big data analytics, and intelligent transportation system.